Post print of the paper published on Journal of Applied
Geophysics 193 (2021) 104407

Subsurface profiling of buried valleys in central alps (northern Italy) using HVSR single-station passive seismic

M. Mele [a,c,*], R. Bersezio [a], A. Bini [a,†], M. Bruno [a], M. Giudici [b], D. Tantardini [a]

[a] *Dipartimento di Scienze della Terra "A. Desio", Universita degli Studi di Milano, via Mangiagalli 34, 20133 Milano, Italy* ` [b] *Dipartimento di Scienze della Terra "A. Desio", Universita degli Studi di Milano, via Cicognara 7, 20129 Milano, Italy* ` [c] *Studio Geo360, Via Trieste 97, 20064 Gorgonzola, Italy*

Keywords:
Ambient seismic noise
Buried valleys
HVSR
Landscape evolution
Geomorphology Central Alps

ABSTRACT

Active and passive seismic techniques permit to draw images of relevant buried morphologies in mountainous areas. Here we apply the Horizontal-to-Vertical Spectral Ratio (HVSR) passive seismic technique to draw the shape of a buried valley in the core of the Italian Central Alps, at the confluence among the fault-controlled Valtellina, Valchiavenna and Lake Como depressions ("Colico knot"). Twenty-three single-station, ambient- noise measurements were acquired and the site-specific fundamental frequency f_0 was obtained by computing the HVSR in the 0.5 Hz to 5 Hz frequency band.

Shear wave velocity (Vs)-versus-depth profiles were computed from the inversion of the HVSR curves, under the assumption of a 1D structure. To limit uncertainty, the results were calibrated by comparison with data from two sources: 1) HVSR profiles acquired in a comparable setting in Valtellina, at a site where estimates of Vs for the seismic basement and cover sediments were available; 2) borehole logs which crossed the sediments above the metamorphic bedrock at the Colico knot site. Independent data were used to constrain the best fit of the experimental HVSR peaks at the Colico knot site, in terms of frequency f_0 and HVSR amplitude, thus retrieving information about Vs variations related to the bedrock versus sediments unconformity.

A SW-NE elongated buried trough, as deep as 150 m below sea-level and up to 2 km wide was drawn from the present-day Adda valley to the Lake Como depression to the South. The morphology of this abandoned and buried course of the Adda river is controlled by active deep-seated gravitational slope deformation along the adjacent mountain slope. The valley was abandoned before the Last Glacial Maximum (latest Pleistocene), plausibly owing to narrowing and uplift induced by deep-seated slope deformation. In fact, the LGM Adda glacier reshaped the valley slopes and the bedrock watershed that separates at present the post-Glacial Adda river course from the paleo-Adda trough.

1. Introduction

The geophysical reconstruction of the subsurface of deep, intra- valley basins in mountain ranges is relevant to understand the present and past dynamics of mountain landscape evolution (Felber and Bini, 1997; De Franco et al., 2009; Maheo et al., 2013; Willett et al., 2006) and finds a wide range of geological, geomorphological and civil applications, specifically for hydrogeology, hazard and risk assessment studies and for the evaluation of site-effects on seismic ground motion due to amplification mechanisms (D'Amico *et al.,* 2008; Panzera et al., 2019).

This task is very challenging, because of the complexity of the buried morphology of these settings, which are characterized by sharp bedrock-sediments edges derived from active deformation processes, slope instability, weathering, erosion processes and deposition of a possibly thick sediment infill. Furthermore, the thickness of the cover sediments represents a relevant limiting factor for the expensive direct investigations, such as borehole drilling.

To map the morphology of the bedrock and to interpret the stratigraphic sequence within intramountain valleys, a wide range of geophysical methods, such as gravity, audio-magneto telluric, resistivity and seismic methods could be applied (Reynolds, 2011).

Seismic prospecting is one of the most widely used techniques in these settings, since lithostratigraphy controls the vertical distribution of the seismic properties (Castellaro et al., 2005) owing to strong contrasts of physical parameters between the bedrock and the infill. In particular, active seismic techniques, such as refraction and reflection methods, can provide the best resolution for a detailed mapping of the bedrock surface (De Franco et al., 2009; Oldenborger et al., 2016; Maraio et al., 2018 and references therein). Unfortunately, their application requires a strong economic and technical effort, in order to plan and execute extensive surveys. Within this framework, passive seismic techniques, namely the single-station horizontal-to-vertical spectral ratio (HVSR) method (Nogoshi and Igarashi, 1971; Nakamura, 1989), is comparatively fast and cheap compared to active methods, because a single light-weighted, broadband seismometer is used and no artificial source is needed, so that valuable results can be obtained, even if some assumption about the underground structure have to be formulated (see Section 3.1). In particular, HVSR surveys can provide a gross image of the depth of major seismic impendence interfaces and can drive the planning of high-definition active surveys.

HVSR method is based on the recording of the amplitude ambient seismic noise wavefield, i.e. microtremors, without the need of any artificial source and any environmental impact. Microtremor is a generic term adopted to represent vibrations measured at the ground surface produced both by natural and anthropic sources (Bonnefoy-Claudet et al., 2006; SESAME, 2004), which cover a frequency band between 0.1 Hz and 100 Hz and whose spectral components are generally poorly attenuated within the Earth. HVSR method uses the seismic microtremor field, recorded in its spatial three-components with a seismometer, to compute the ratio between the spectral component of the wavefield in the horizontal plane and in the vertical direction.

In recent years, HVSR method has been increasingly applied to seismic risk assessment and studies of amplification at local scale (Foti et al., 2011; Lunedei and Albarello, 2010; Martorana et al., 2017) and to map the thickness of relatively low-velocity sedimentary sequences inside basins (Bonnefoy-Claudet et al., 2009; Borges et al., 2016; D'Amico *et al.,* 2004; Gosar and Lenart, 2010; Hinzen et al., 2004; Mahajan and Praveen, 2018; Yamanaka et al., 1994). When a calibration of the shear wave propagation velocity (Vs)-versus-depth profile is available, the method permits to retrieve the average Vs in the shallowest portion of the subsoil, which is related to its mechanical characteristics and vertical compaction, controlling the frequency band and amplitude of seismic wavefield emerging at the ground.

In the case of an intra-mountain valley, where stiff terrains or fractured rocks lie above and aside a hard bedrock, which is a relatively high-velocity target for classical refraction and reflection methods due to the strong seismic

* Corresponding author at: Dipartimento di Scienze della Terra "A. Desio", Universita degli Studi di Milano, via Mangiagalli 34, 20133 Milano, Italy. ` *E-mail address:* mauro.mele@unimi.it (M. Mele). † Deceased author.

https://doi.org/10.1016/j.jappgeo.2021.104407

impedance contrast, a HVSR peak might be depicted. Under these conditions and based on some needful simplification on the nature of the seismic microtremor wavefield and on the geometry of the buried morphology, the frequency and the amplitude of the HVSR peak could be used to roughly estimate the depth of the impedance contrast and the average shear-wave velocity properties across the seismic discontinuity.

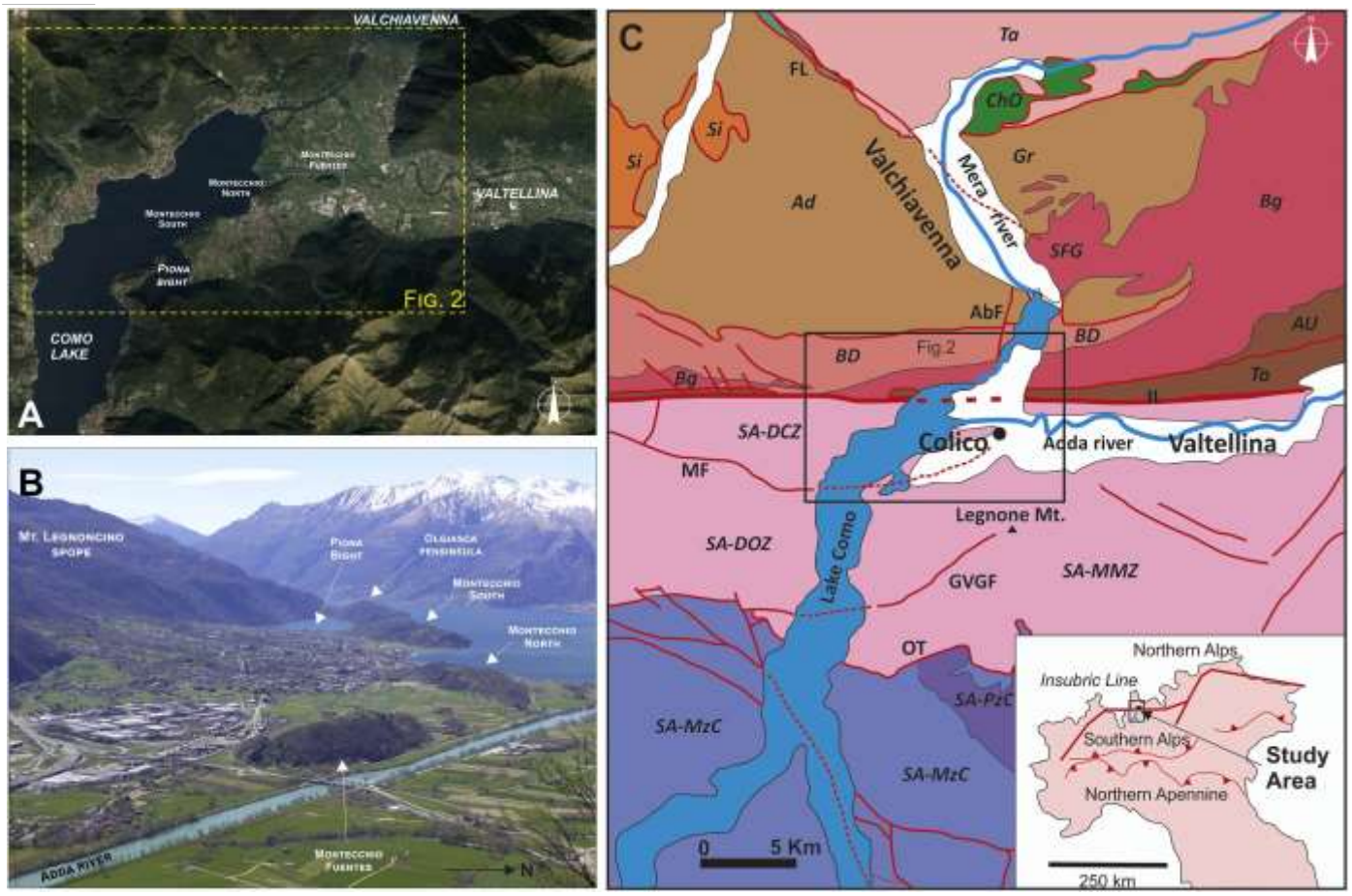

Fig. 1. A) aerial view of the Colico knot. B) the Montecchi area as seen from the northern mountainside of Valtellina. C) Location and structural map of the Colico hydrographic, geomorphological and geological knot. Southern Alps: SA-DCZ, Domaso-Cortafo Zone; SA-DOZ, Dervio-Olgiasca Zone; SA-MMZ, Monte Muggio Zone; ` MF, Musso fault; GVGF, Grona-Val Grande fault, OT: Orobic thrust; SA-PzC: Paleozoic Cover; SA-MzC: Mesozoic Cover. Penninic System: AD, Adula Nappe; Gr: Gruf complex; Si: Simano Nappe; BD, Bellinzona-Dascio Zone; ChO: Chiavenna Ophiolite. Austroalpine System: To, Tonale Gneiss (Upper Austroalpine); AU: Austroalpine Nappes. Tertiary Intrusives: Bg, Bergell Pluton; SFG, San Fedelino Granite – Novate Mezzola Swarm. IL: Insubric line; AbF: Albonico fault scarp, FL: Forcola line. Compiled and redrawn after Montrasio et al. (1990), Bigi et al. (1990), Tibaldi and Corazzato (2001), Spalla et al. (2002), Geologische Carte der Schweiz (2005).

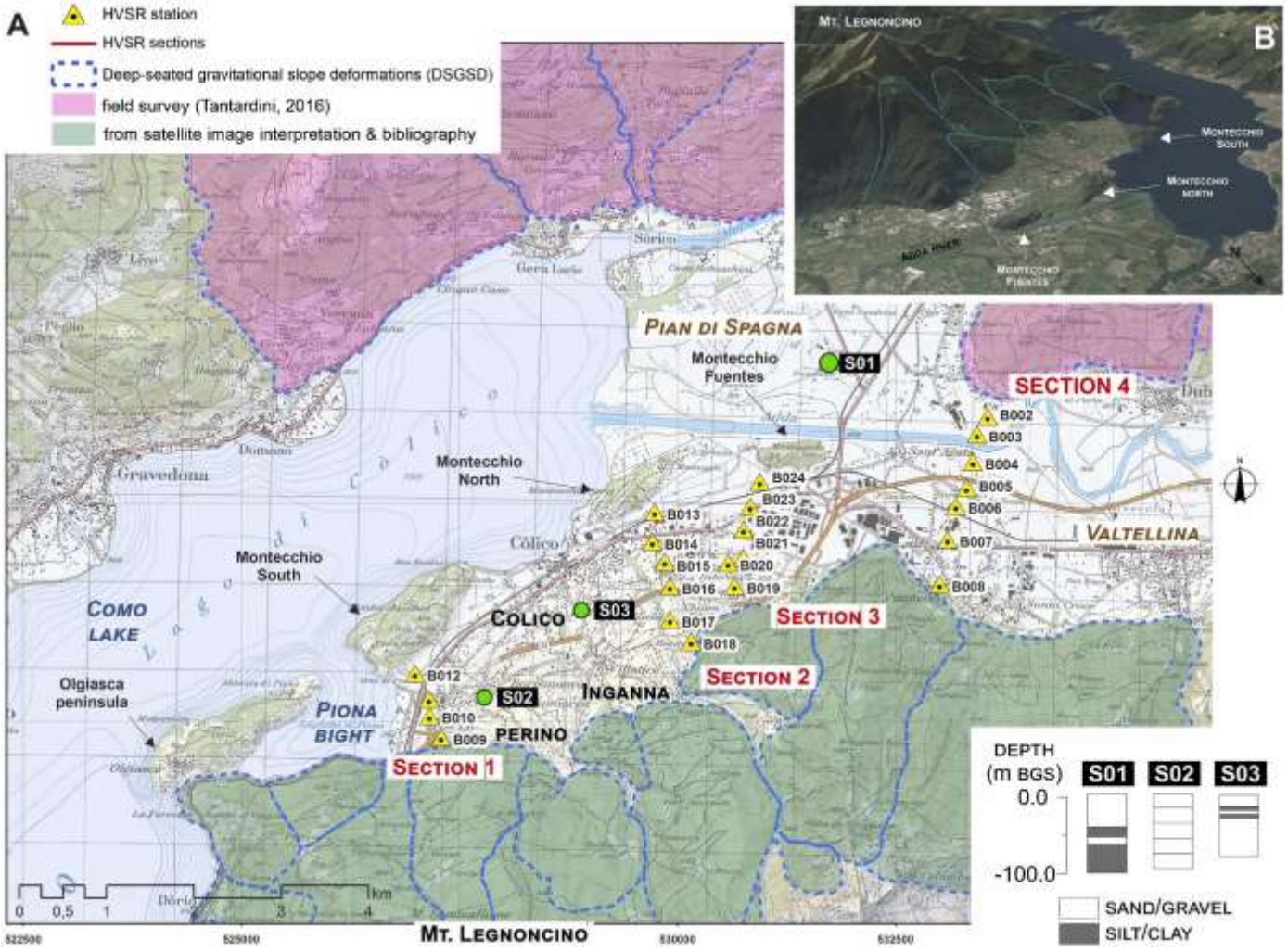

Fig. 2. Box A: Map of the HVSR stations and sections (location of the map in Fig. 1A): yellow triangles represent the sites of the 23 measuring stations. Green dots represent boreholes logs (simplified lithological logs are shown in the lower-right corner box; white as sand/gravel, grey as silt-clay). Box B: aerial view of the northern flank on Mt. Legnoncino; the boundaries of the deep-seated gravitational slope deformations are drawn in blue, as in the main map of box A (image from Google Earth, view from NE to SW). (For interpretation of the references to colour in this figure legend, the reader is referred to the web version of this article.)

1.1. Target area and aims

In this study, we evaluate the application of single-station passive seismic surveys to the reconstruction of the morphology of the buried bedrock top at the eastern end of the intra-mountain valley of the Adda river ("Valtellina"), a prominent valley of the Central Alps, in Northern Italy. The target area (Fig. 1) is the sector where Valtellina, Valchiavenna (the Mera river valley) and the depression nowadays occupied by Lake Como merge in a sort of triple point (Fig. 1c) near the Colico town. The relevant morpho-structural significance of this triple junction suggests the definition of "Colico knot", which is adopted in this paper.

The area shows several geological and geomorphological examples of the complex landscape evolution of the Central Alps. It represents a hydrographic, geological and geomorphological key-zone because of its polygenetic and complex evolution, since the entrenchment of the well- known Messinian buried canyon which was detected below the present- day Plio – Quaternary, glacio-lacustrine sedimentary infill of Lake Como depression (Bini et al., 1978, 1994; Finckh, 1978; Finckh et al., 1984).

Besides the evaluation of the HVSR method for such a setting, the work aims to assess the likely existence of a buried, abandoned branch of the Adda valley, documenting a past configuration of the Colico knot, somewhat different from the present-day setting. The attempt is to add circumstantial evidence to the geomorphological and geological evidences suggesting that an ancient Adda valley could have run close to the present-day SE slope of Lake Como (Fig. 1b), and that the Mera – Adda confluence might have occurred southwards than at present, south of the Piona bight (Fig. 1a).

To this purpose, 23 ambient-noise measurements at the Colico knot have been acquired and processed. The geophysical interpretation of these data was obtained by 1D inversion and one of the major geophysical challenges of this work was the uncertainty in HVSR inversion. In order to obtain reliable models of the subsurface, we chose to constrain the parameters of seismic models (V_S-versus-depth profile) by using information from other geophysical and geological, independent data. First, an area in Valtellina, where an independent seismic data-set was acquired with the seismic reflection method (De Franco et al., 2009), was considered as an analogue of the area surveyed with the present work. Then, two HVSR stations were collected there and the results of the migrated seismic section by De Franco et al. (2009) were used to fix the depths of the main discontinuities. As a consequence, reliable estimates of the ranges of shear-waves propagation-velocity in different media were obtained. Second, lithological borehole logs down to a depth of about 100 m from the ground surface that are available in the study area were used to constrain the inversion for relatively shallow structures.

Furthermore, for inversion, also the shape of the HVSR peaks was considered, as the difference between sharp and wide peaks could correspond to different geometrical structures and to different lateral and vertical variability of physical parameters. Obviously, this is of paramount importance for the final geological interpretation.

2. Geology and geomorphology of the Colico knot

2.1. Regional setting

The Colico knot develops across and south of the Insubric line (Fig. 1c), the lithospheric fault which joins the Austroalpine and Penninic nappes of the Central Alps (to the North) with the basement- involved thrust system of Southern Alps (to the South; Bigi et al., 1990). At the knot, Valtellina and Valchiavenna meet to form the Lake Como valley.

The southern end of Valchiavenna runs across the Penninic System, here represented by the Adula Nappe (Milnes and Pfiffner, 1980) and the Bellinzona-Dascio Zone (Montrasio et al., 1990, 1994; Geologische Carte der Schweiz ,2005; Fig. 1) and cuts through the steeply dipping "root" zone of the Alpine nappe system (Austroalpine, Tonale Gneisses) which form a thin, nearly vertical slice parallel to the Insubric line (Schmid et al., 1989; Montrasio et al., 1994). Valchiavenna is a fault-controlled valley. North of the Novate-Mezzola dyke swarm (Fig. 1c) it strikes NNW-SSE, parallel to the Forcola normal fault (Ciancaleoni and Marquer, 2008). Its southernmost segment turns to NN*E*-SSW parallel to the Albonico fault (Tibaldi and Corazzato, 2001), then merges with the northernmost straight branch of the Lake Como valley (Fig. 1c).

Valtellina runs E-W parallel to the Insubric line, almost normal to Lake Como (Fig. 1c). To the South of it, the Southalpine basement of the Colico knot comprises three tectono-metamorphic units (Domaso- Cortafo Zone, DCZ; Dervio-Olgiasca Zone, DOZ; Monte Muggio Zone, ` MMZ) bounded by two prominent fault zones which played a relevant morphogenetic role in the knot, together with the Insubric line: the Grona – Val Grande fault and the Musso fault (Fig. 1c; Milano et al., 1988; Bini et al., 1994; Spalla et al., 2002). The three tectonic units are mostly formed by the so-called Morbegno Gneisses, an association of micaschists and gneisses with minor interlayered amphibolite, quartzite, marble, calcschists and meta-granitoids with some pegmatites occurring in the DOZ only (Spalla et al., 2002). These rocks are expected to form the seismic bedrock of the inferred Adda buried valley.

The N-S solitary segment of the Lake Como valley cuts obliquely the mentioned boundaries of the Southalpine tectonic units (Fig. 1c). Its northern termination is diverted to NE-SW strike at the Colico knot, between the Musso fault and the Insubric line (Fig. 1c). Below the sedimentary fill of the Lake Como Messinian canyon (Bini et al., 1978), the top of the bedrock deepens progressively from − 537 m to − 886 m below sea-level south of the Grona–Val Grande fault (Finckh, 1978; Fig. 1c). The sediments-over-basement contact is likely to step-up across the fault, as it is suggested also by the bathymetric sill of the lake floor at 140 m above sea-level (Menaggio – Bellagio plateau, Fanetti et al., 2008). This hinge connects the bifurcate southern segment of Lake Como, characterized by a deep sedimentary bedrock top, to the solitary northern segment of the Lake (Fig. 1c). Between the Grona–Val Grande fault and the Insubric line, the Southalpine metamorphic basement is buried by the canyon sediments at a much shallower depth than southwards. A second step in the bedrock top might occur across the Musso fault, which intersects the Lake Como depression in correspondence of the Olgiasca peninsula and bounds the Piona bight (Fig. 1c and Fig. 2); this remark suggests that the depth of the bedrock top might be even shallower. Reflection seismic sections (Finckh et al., 1984) showed that the valley flanks continue into the lacustrine sub-bottom with about the same slope, down to the bedrock top. According to Finckh (1978), the 460-m-thick sediment fill at the northern tip of the bifurcation of the lake (Fig. 1) consists of post-glacial and Holocene lacustrine fines with mass gravity flow and landslide deposits (Fanetti et al., 2008) resting above water-saturated alluvial and glacio-fluvial gravels and sands with till which cover the lowermost staff consisting of partly cemented gravels and sands.

2.2. Geological clues of a buried Adda valley at the Colico knot

At the northern end of Lake Como, the prograding post-glacial delta plain of the Adda river forms a wide, flat plain, corresponding to the present-day Pian di Spagna (Fig. 1 and Fig. 2). The relics of a NE-SW smoothed rock crest between Valtellina and Valchiavenna emerge from the delta plain, forming the Montecchio di Fuentes, Montecchio N, Montecchio S and Olgiasca peninsula line-up, from NE to SW (Fig. 1b and Fig. 2). These sheepback-shaped spurs roughly correspond to the greenschist mylonitic belt that parallels the boundary between the DCZ and the DOZ, along the Musso line (Chinaglia and Soldo, 1994; Bini et al., 1994; Spalla et al., 2002; Fig. 1c). The elongation of the individual spurs and their alignment broadly parallel the main regional foliation, that dips between 65° and 80° to SSE and/or NNE, coherently in the spurs and on the slopes of Mt. Legnoncino – Mt. Legnone to the SE (Chinaglia and Soldo, 1994; Bini et al., 1994; Fig. 1 and Fig. 2). The prolongation of this alignment into the present-day watershed between Valchiavenna and Valtellina (Mt. Bassetta – Mt. Foffricio crest, North of Dubino, Fig. 1 and Fig. 2) across the present-day course of Valtellina, is apparent (Nangeroni, 1971). From these features Bini et al. (1994) interpreted the existence of an ancient (Messinian?) watershed between Valtellina and Valchiavenna. As a consequence, an Adda river abandoned valley might have flanked to the NW the Mt. Legnone – Mt. Legnoncino slopes and the confluence between the ancient Mera and Adda Valleys might have occurred to the SW of the Piona bight (Fig. 1 and Fig. 2).

At present, the possible site of the paleo-valley is a topographic depression, whose width is comprised between 1 km and 2 km, occupied from SW to NE, by: i) the Piona bight of Lake Como, with a water depth of about 80 m, to be compared with the water depth of the Lake around the Olgiasca peninsula (about 250 m), ii) the debris flow fans of the Inganna and Perino creeks in the Colico area (Fig. 2) and iii) the Adda lacustrine delta plain sediments of the Pian di Spagna (Fig. 2).

Boreholes and water wells near Colico (S02 and S03 in Fig. 2) crossed a succession of alluvial gravels and sands interfingered with lacustrine fines, forming one or two progradation cycles, down to some 100 m below the ground surface. A comparable succession can be reconstructed at the north-eastern side of the Pian di Spagna (present-day Adda delta plain) where borehole S01 was drilled down to 100 m below ground surface (b.g.s. from now on) (Fig. 2).

Glacial deposits of LGM age (mostly tills belonging to the Cantù Synthem; Bini et al., 1994) discontinuously mantle the mountain slopes around the Colico knot. The LGM trimline is located at 1690 m a.s.l. on the northernmost slope of Lake Como (Mt. Berlinghera and Mt. Sasso Canale; Tantardini, 2016), at 1805 m a.s.l. on the Mt. Bassetta – Mt. Foffricio crest and on the Mt. Legnone northern slope (Pedroncelli, 2013; Tantardini, 2016). LGM glacial morphologies have been reported at several locations, like on the western slope of Mt. Legnoncino (sloping toward the Piona bight; Bini et al., 1994; Fig. 2) where the glacial trimline runs at 1510 m a.s.l. (Tantardini, 2016). At this site, sheepback rocks also occur inside and across the scarp of the Mt. Piazzo landslide and trenches, suggesting that it predates the LGM (Chinaglia and Soldo, 1994; Bini et al., 1994).

Deep-seated gravitational slope deformations (DSGSD) widely affect the region. The distribution of sackung-related morphologies on the slopes bounding the Colico knot is shown in Fig. 2, after Tantardini (2016). The relation between structural features and DSGSD is tight in the study area, where trenches, scarps, counterscarps and most of the sackung-related morphologies (Fig. 2b) are clearly controlled by the dip of the regional foliations (N- versus S- steeply dipping S2 in the Southalpine side of the Colico knot) and/or by faults and joints (southernmost Valchiavenna, Albonico scarp, Tibaldi and Corazzato, 2001; Fig. 1 and Fig. 2). In the case of Mt. Legnoncino sackung, several lines of evidence led Chinaglia and Soldo (1994) and Ambrosi and Crosta (2006) to recognize the ongoing deformation of the NW Mt. Legnoncino flank, whose inception predates the LGM (Bini et al., 1994). According to Bini et al. (1994), the Olgiasca peninsula was a stable relief, detached, separated and independent from the Mt. Legnoncino slope. The pre-LGM DSGSD slow motion would have been responsible for closing of the Piona bight and for the origin of the topographic link between the Olgiasca peninsula and the Mt. Legnoncino slope, as it is observed at present.

Fig. 3. ambient seismic noise acquisition at site B004 (location in Fig. 2) with PASI Gemini equipment.

3. Methodology

3.1. HVSR method

HVSR method is based on the recording of the vertical and horizontal components of the ambient seismic noise wavefield, the computation of the Fourier transform and of the ratio between horizontal and vertical spectral components of the ground motion at every investigated frequency.

When energy (from both natural and anthropic sources) travels in the ground in the form of microtremors, the heterogeneity of the subsurface produces different interference effects on the horizontal and vertical components of the seismic waves. In the simplest case of a single discontinuity between laterally homogeneous layers and for an isotropic seismic noise, a HVSR peak should be detected. In recent literature, there is a general agreement about the dual nature of sources of the seismic noise wavefield between 0.1 Hz and 100 Hz: natural sources at low frequencies, such as ocean and large-scale meteorological conditions; anthropic sources at higher frequencies (Gutenberg, 1958). Yet the composition of the seismic noise wavefield (Lunedei and Malischewsky, 2015 and references therein) and different physical models of the HVSR behaviour (body or surface waves) are still debated (Mi et al., 2019; Pina-Flores et al., 2016 ˜ and references therein).

Within this general frame, a wide literature shows the close link between the noise wavefield, the subsurface seismic structure (mainly driving the shear waves properties affecting wave propagation) and the HVSR peak interpretation. With a simple two-layers seismic structure (Arai and Tokimatsu, 2004; Lunedei and Albarello, 2010), a HVSR peak occurs at a frequency f_0 (fundamental resonance frequency of the site) directly proportional to V_S of the overlying medium and inversely proportional to the depth of the high-velocity bedrock (h): $f_0 = V_S (4\ h)^{-1}$ (Yamanaka et al., 1994). Furthermore, since the superposition of stiff terrains (sediments and/or fractured/weathered rocks) above a hard bedrock reasonably represents a two-layers seismic structure, sharp peaks represent proxies of sharp contrasts of elastic parameters (Tarabusi and Caputo, 2017), thus retrieving information on the corresponding seismic discontinuities.

From a general point of view, it should be stressed that the inverse problem in surface-wave analysis is nonlinear and it suffers from solution non-uniqueness so that, when only f_0 is known from an ambient seismic noise measurement, an infinite number of 1D synthetic models (i.e., Vs-versus-depth profiles) could be proposed to fit the HVSR peak, both in terms of frequency and amplitude (Castellaro and Mulargia, 2009).

Therefore, when applying the HVSR method to subsurface profiling from single-station measurements, constraints on Vs and/or infill thickness from independent methods are necessary to limit the interpretation uncertainties on the model used to fit frequency and amplitude of the peak (Barnaba et al., 2010; Paolucci et al., 2015).

Moreover, in the case of buried valleys where the approximation of 1D geometries is weak, the reliability of f_0 values emerging from HVSR data must be evaluated under the light of possible resonance effects on the recorded seismic noise wavefield produced by the complex, 2D/3D buried geometries in the subsurface.

These effects are generally very difficult to evaluate in the experimental evidences, but promising results from numerical modelling show that they could correspond to a larger signal duration, that overestimates the real f_0 at the site (Roten et al., 2006; Gu´eguen et al., 2007), and an amplitude of the HVSR peak lower than that predicted for 1D structures (Bard and Bouchon, 1985; Mozco and Bard, 1993; Guillier et al., 2006; Le Roux et al., 2012).

From a diagnostic point of view, when the 1D assumption is valid, HVSR plausibly shows a narrow, well-defined peak, especially when large seismic impedance contrasts are present (Le Roux et al., 2012), so that the relation between f_0, average Vs and thickness of the valley infill could be applied (Yamanaka et al., 1994). On the other hand, when irregular bedrock morphology and/or abrupt basin edges are present, complex HVSR peaks appear, due to resonance effects. In some case, it is reported that a broad-band, plateau-like HVSR peak with small amplitude could be found at these site (Guillier et al., 2006; Bonnefoy-Claudet et al., 2009).

Notice that during the investigation of buried valleys with complex shapes, different conditions could be met at different points within the same valley: areas where the 1D approximation is reasonable and HVSR curves show sharp

peaks and areas where HVSR curves are heavily influenced by the effects of 3D features of the geological structures,

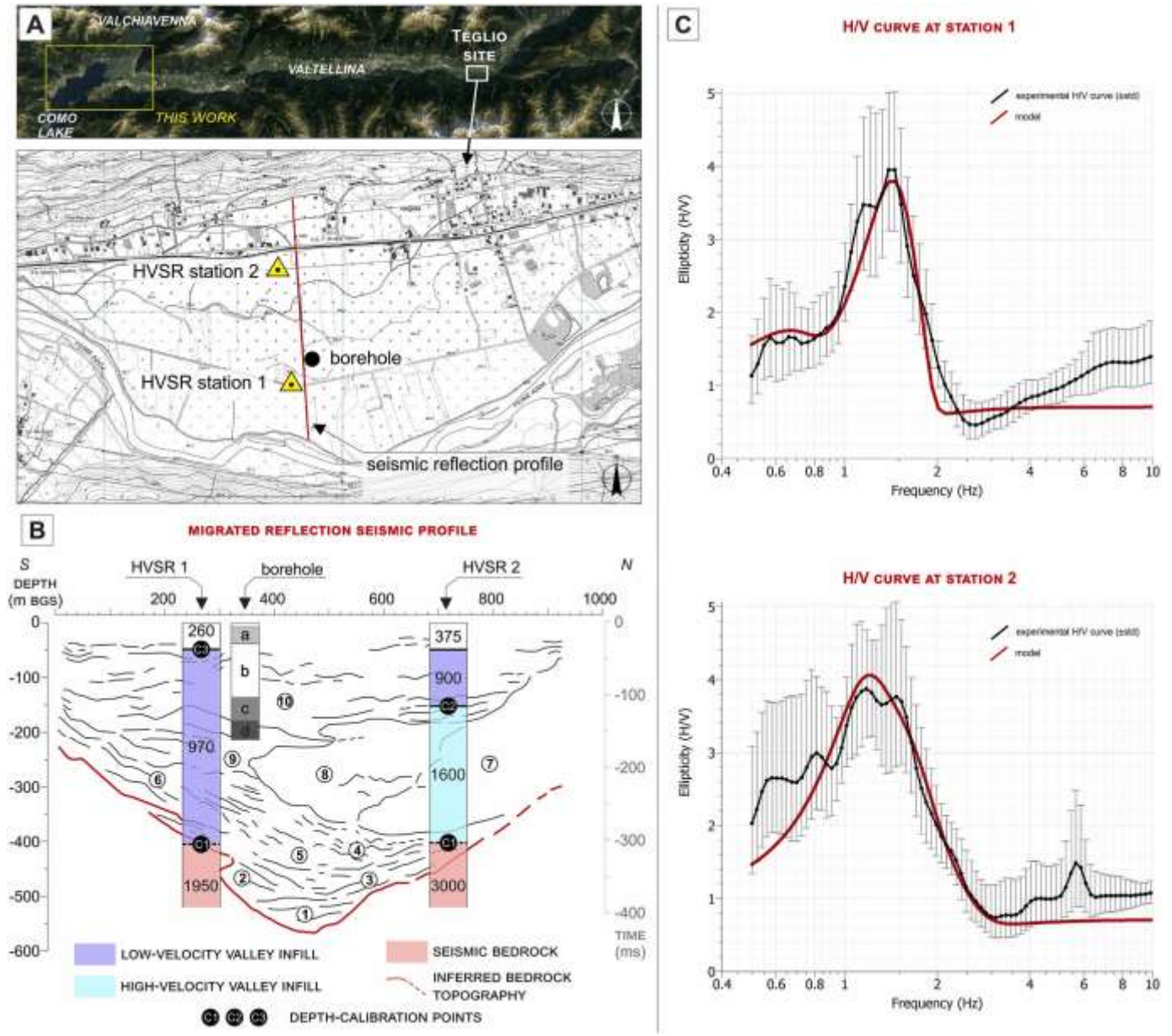

Fig. 4. HVSR data calibration at the Teglio site (Box A). Box B: Vs profile obtained at HVSR 1 and HVSR2 stations superimposed to the line-drawing of the Teglio depth-migrated reflection profile (interpreted after De Franco et al., 2009) and the seismic bedrock from the Authors (red line). Numbers from 1 to 10 refers to: (1) lacustrine deposits; (2, 3, 4, 5, 6) slope and fluvial deposits; (7) DSGSD mass; (8,9) slope deposits; (10) fluvial to lacustrine deposits. Depth-calibration points C1÷C3 are shown in black. Box C: HVSR curve obtained at station HVSR 1 and 2 and curve-fitting.

which correspond to a complex variation of physical parameters, i.e., density and Vs (Guillier et al., 2006; Le Roux et al., 2012).

3.2. Survey design and data acquisition at the Colico knot

Ambient seismic noise was recorded at 23 stations in the Colico knot as shown in Fig. 2, taking care to avoid the areas with intense anthropic activity (Fig. 3). The covered area is approximately 11.4 km^2 for a corresponding station density of 2 stations per square kilometer. The seismic signal was recorded for the three orthogonal components (one vertical, Up-Down; two horizontal N-S and *E*-W) in free-field conditions, with the 3D land geophone PASI GEMINI with an eigenfrequency of 2 Hz and 24-bit data acquisition board (Fig. 3).

According to the SESAME (2004) guidelines, the sensor was coupled with the ground, taking care to protect it from wind and to partially bury it, for approximatively a half of its height, in order to fix a stable and horizontal position (Foti et al., 2017), with a N-S and E-W alignment of the horizontal sensors. The minimum recording time for each station was 30 min, with a sampling rate of 5 ms (sampling frequency of 200 Hz).

The 23 stations were located at sites far from buildings, power lines, other potentially interfering infrastructures and tall trees. The high density of infrastructures and settlements did not permit to distribute the stations uniformly over the study area, and therefore four transects were designed to cover almost all the sub-areas, where reliable measurements could be obtained following the SESAME (2004) indications (Fig. 2). The horizontal separation between two adjacent stations along the transects is always less than 500 m, in agreement with the deployment of measurements in similar recent studies (Mantovani et al., 2019). Recent results show that this spacing is acceptable to image structures at large scale (see, e.g., Fig. 5 of Mantovani et al., 2018, and Fig. 7 of Tarabusi and Caputo, 2017), whereas fine scale features could remain undetected or could be aliased. This acquisition plan permitted to obtain four pseudo-2D sections after interpolation of the local 1D models. The four transects were oriented perpendicular to the presumed

buried valley axis, to extend in the subsurface the exposed contour of the bedrock-sediments contact and to account for the mapped geomorphological features of both valley-flanks. The integration of HVSR pseudo- 2D sections with the geological and geomorphological constraints (Fig. 2, Section 2.2) permitted to draw the subsurface interpretation that is sketched for an immediate readability by a smoothed contour map of the presumed depth of the bedrock-sediments interface (Section 4.2).

Three transects were located between the NE flank of Mt. Legnoncino and the Montecchi and oriented approximately from NNE-SSW to NNW- SSE: section 1, stations from B_009 to B_012 between Montecchio South and Mt. Legnoncino; section 2, stations from B_013 to B_018 between Montecchio North and Mt. Legnoncino; section 3, stations from B_019 to B_024 between Montecchio di Fuentes and Mt. Legnoncino (Fig. 2). A further transect (section 4, stations from B_002 to B_008) was located at the western margin of Valtellina and is oriented NNE-SSW (Fig. 2).

3.3. Data calibration: The reference Teglio site

In order to constrain the HVSR peak inversion to obtain Vs-versus- depth profiles at the Colico knot (see next Sub-section 3.4 for details), a published reference case-study in a comparable geological and geomorphological setting of Valtellina was considered to achieve a set of reference values for Vs (De Franco et al., 2009).

The basic idea was to calibrate the HVSR peaks at a study site where an independent seismic data-set is available. To this purpose, we focused on the seismic reflection profile obtained by De Franco et al. (2009) at the Teglio site, in the eastern part of Valtellina (Fig. 4a), some 50 km East and uphill from the Colico knot. Here, a depth-migrated, reflection seismic profile was calibrated to a lithological borehole log down to 200 m b.g.s., in a bedrock/sediment setting comparable to the Colico knot site (Fig. 1 and Fig. 2). At the Teglio site, Valtellina is approximately 1200 m wide and the seismic basement is interpreted at about 550 m below the ground surface. The seismic basement is characterized by a P- wave velocity larger than 3200 m/s, in contrast with the overlaying sedimentary sequence characterized by an average P-wave velocity of 1400 m/s (De Franco et al., 2009).

The shallow part of the section (Fig. 4b; less than 200 m b.g.s.) shows horizontal reflectors, which pinch out toward the northern and the southern flanks of the valley. These are interpreted as due to a complex interfingering of Quaternary alluvial, glacial and lacustrine deposits (De Franco et al., 2009). At increasing depth, at the northern valley flank, a thick and curved set of reflectors dips toward the valley centre: the high- amplitude of this set (see marker number 7 in Fig. 4b) suggests the presence of a rocky mass, up to 300 m thick, that occupied a former paleo-valley. At the southern flank and in the centre of the valley, low- amplitude reflectors below the high-amplitude set suggest stiff material, plausibly slope, fluvial and lacustrine deposits laying above the seismic basement/bedrock (see marker number from 1 to 5 in Fig. 4b; De Franco et al., 2009). The seismic image of the Teglio site shows a southern valley side where the stiff sediments directly cover the seismic bedrock, which contrasts with the northern valley flank where a rocky mass is interposed within the sedimentary fill laying above the seismic bedrock (Fig. 4b).

In order to profit from the two different settings shown by the seismic line on the opposite sides of the valley, two ambient seismic noise measurements (Fig. 4b, c) were acquired. Two HVSR curves with sharp f_0 peaks were obtained in the range between 0.5 Hz and 2.0 Hz, with an amplitude of the HVSR at f_0 up to 4.

Based on these features, the HVSR curve-fitting was performed in the 0.5 Hz to 5 Hz frequency band (see Section 3.4 for processing details), by assuming the presence of seismic impedance contrast between the near- surface sediments, the interposed rocky mass, the underlying sediments and the local bedrock.

Three depth-calibration points were used to constrain the data inversion:

- the depth of the rocky bedrock, obtained by the seismic depth- migrated profile (400 m b.g.s.; C1 at both HVSR1 and HVSR2 sites in Fig. 4b);
- the depth of the top of the interposed rocky mass in the northern flank, obtained by the seismic depth-migrated profile (150 m b.g.s.; C2 at HVSR2 site in Fig. 4b);
- the depth of the transition between sand layers (fluvial deposits) and matrix supported diamicton (glacial deposits), described in the lithological log at shallow depth (400 m b.g.s.; C3 at HVSR1 site in Fig. 4b).

To obtain a good match between the experimental HVSR curve and the modelled one at each site, a three-layer model was used for HVSR curve at station 1 and a four-layer model for HVSR curve at station 2.

A good agreement between the experimental and modelled HVSR was obtained (Fig. 4c), hence the reference values for Vs of the basin infill at the Teglio site were estimated in the following ranges:

- from 260 m/s to 753 m/s and from 900 m/s to 970 m/s respectively for the shallow and the deep part of the valley infill at the southern flank (sediments above and below the rocky mass and slope deposits);
- about 1600 m/s for the rocky mass (DSGSD and slope deposits) in the northern flank;
- $>$ 1950 m/s for the bedrock.

The Vs values obtained for the sedimentary infill are quite similar to those proposed at other intra-valley basin settings (Civico et al., 2017; Gu´eguen et al., 2007). The estimated Vs for bedrock, considering an average Poisson's ratio of 0.25 (Reynolds, 2011), reasonably corresponds to the average P-wave velocity greater than 3200 m/s proposed for the metamorphic bedrock of the Central Alps (De Franco et al., 2009).

Regarding the nature of HVSR peaks, with the previous assumption it should be noted that experimental f_0 peaks are not likely related only to the impedance contrast between the bedrock and the infill, but also to the contribution of shallower interfaces within the infill, as it was reported in other basins (Civico et al., 2017).

Finally, if the valley infill includes a large rocky mass interposed within the sediments at the northern valley side, a strong variation of the physical properties with respect to overlying materials (Fig. 4b) and a strong lateral Vs variation are expected in the intermediate infill. This might justify the sharp HVSR peaks (Fig. 4c), which are typical of a 1D structure (Guiller et al., 2006).

3.4. HVSR data analysis and inversion at the colico knot

The analysis of HVSR data at both the Colico knot and the calibration Teglio site consisted of two phases: 1) the computation of the ratio between the horizontal and vertical components of the seismic signal (HVSR curve) and 2) the inversion of the HVSR curve. At the first step, HVSR was calculated with the software GEOPSY (Wathelet, 2006). The software breaks up the signal in time windows of selected length (40 s, in our case); then, after detrending, those segments with a stationary signal were selected, thus eliminating the strong transitory noises (e.g., due to impulsive or local anthropic sources) that are likely to produce spurious HVSR peaks and to reduce the signal-to- noise ratio.

The smoothed spectral amplitude of the three components of the seismic signal was calculated with the application of the Fourier transform in each window and the HVSR was extracted by considering the vertical component (Up-Down) and the average between the two orthogonal components in the horizontal plane (N-S and *E*-W

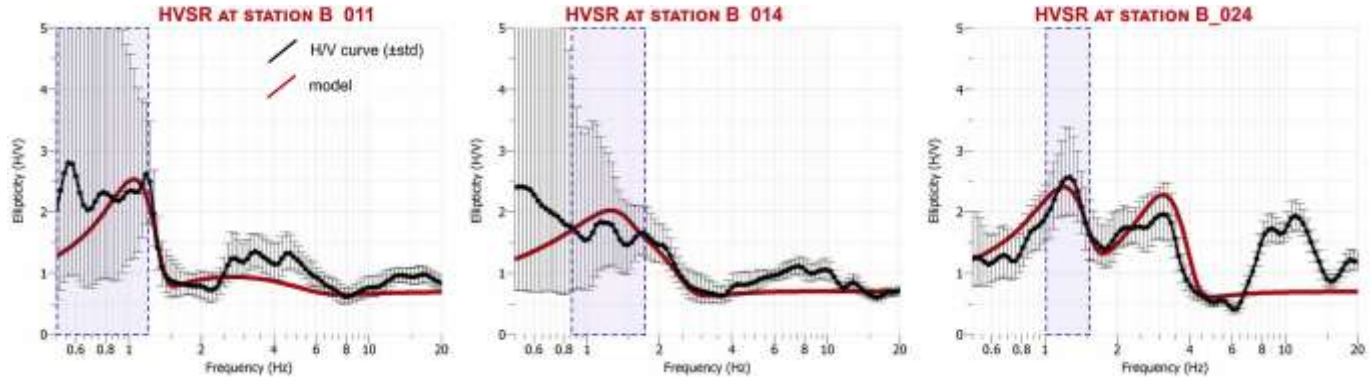

Fig. 5. HVSR curve matching at stations B011, B014 and B024, which are representative of different shapes of HVSR peaks (B011, plateau-like; B024, narrow-peak; location in Fig. 2). (For interpretation of the references to colour in this figure legend, the reader is referred to the web version of this article.)

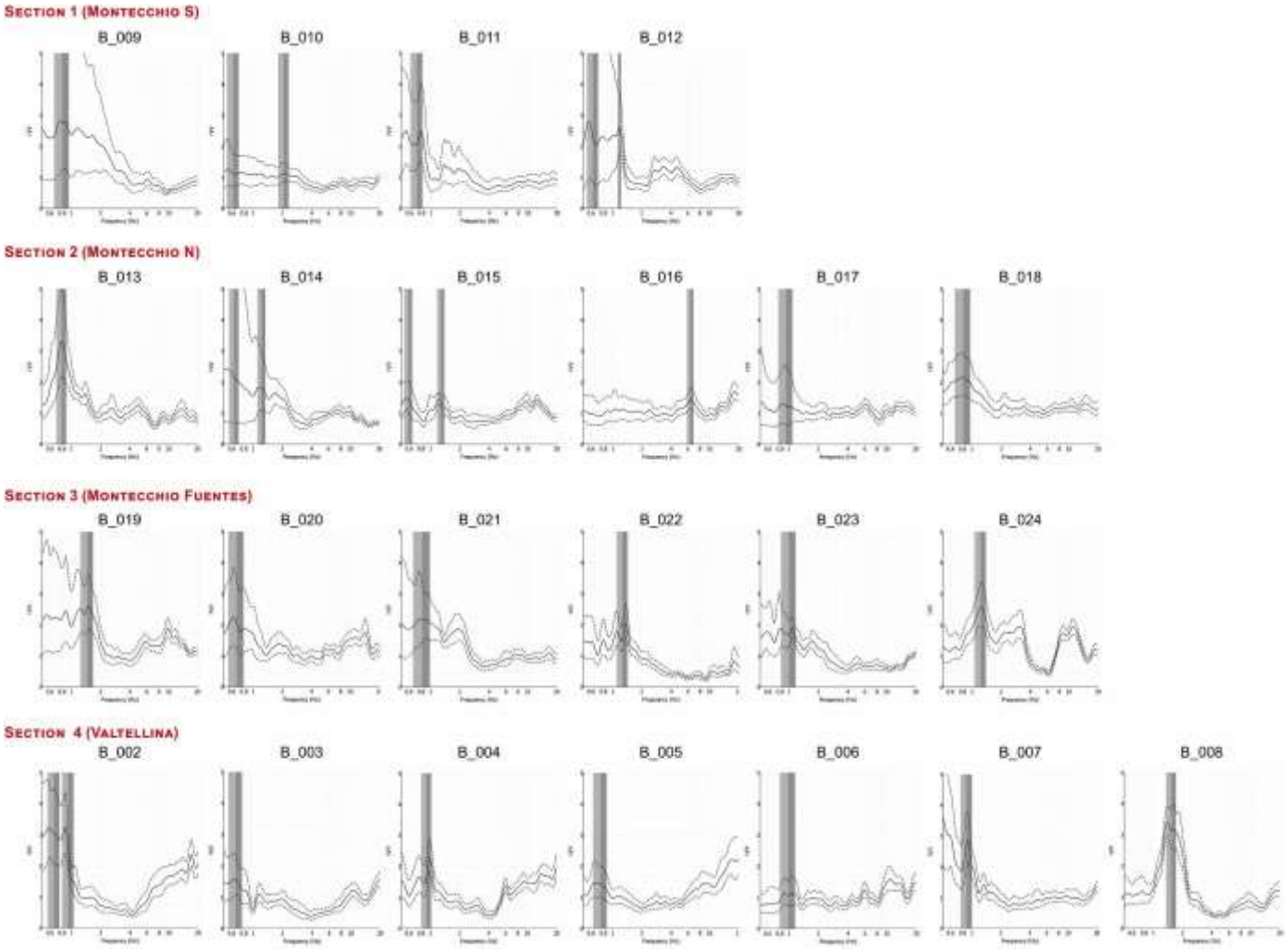

Fig. 6. HVSR curves obtained along the seismic transects shown in Fig. 2. Grey areas identify the HVSR peaks.

components). The average HVSR of each window resulted in a HVSR curve, also called ellipticity curve (black curves in Fig. 4 and Fig. 5), which represents the final HVSR from 0.5 Hz up to 100 Hz.

As a second step, the ellipticity curves previously extracted underwent the inversion process with the module DINVER of the Geopsy package, to identify for each measurement station, a set of seismic models (V_S-versus-depth profile) for which the synthetic ellipticity curve (red curves in Fig. 4 and Fig. 5) is similar to the measured one. To perform data inversion, the reference values for Vs of basin infill and bedrock obtained at the Teglio site were inserted in a first-guess, two- layers model.

The models belonging to the bundle of Vs-versus-depth profiles of each station are equivalent in the sense that the corresponding synthetic HVSR curve overall fits the field curve. The selection of the most likely model from each of these ensembles has been carried out by considering the peaks of the HVSR curves and their characters. In fact, well-defined,

Table 1

Shape and f_0 frequency peaks obtained at the Colico knot (see. Fig. 2 and Fig. 9 for location). N/A stands for "not apparent".

section	ID	peak type	f_0 (Hz)	section	ID	peak type	f_0 (Hz)

1	B009	plateau	0.8 ± 0.14	3	B019	plateau	1.46 ± 0.22
	B010	narrow	N/A		B020	narrow	0.68 ± 0.12
	B011	plateau	0.72 ± 0.1		B021	narrow	0.82 ± 0.16
	B012	plateau	1.17 ± 0.05		B022	narrow	1.26 ± 0.17
2	B013	narrow	0.79 ± 0.09		B023	narrow	0.99 ± 0.17
	B014	narrow	1.22 ± 0.12		B024	narrow	1.23 ± 0.16
	B015	narrow	1.28 ± 0.11	4	B002	plateau	0.92 ± 0.13
	B016	plateau	N/A		B003	narrow	0.66 ± 0.1
	B017	narrow	0.92 ± 0.15		B004	narrow	0.91 ± 0.11
	B018	narrow	0.81 ± 0.15		B005	narrow	0.75 ± 0.12
					B006	plateau	N/A
					B007	narrow	0.88 ± 0.12
					B008	narrow	1.53 ± 0.17

narrow HVSR peaks with f_0 between 0.5 Hz and 5.0 Hz were fitted in such a way as to reproduce both the frequency and amplitude of the peak (Fig. 5); on the other hand, for broadband, plateau-like peaks, f_0 only was fitted, by targeting the frequency at the plateau cut-off (Guillier et al., 2006; Le Roux et al., 2012), whereas the amplitude of HVSR was not considered because it is poorly sensitive. HVSR peaks at high frequency, which appeared in some of the HVSR curves, were interpreted as noise from man-made sources and therefore not considered in this analysis.

4. Results

4.1. HVSR curves and f_0 peaks

HVSR curves obtained along the four sections are shown in Fig. 6. A variety of shapes of f_0 peaks is apparent, from narrow to broadband, plateau-like peaks (Table 1), testifying heterogeneity and complexity in the subsurface of the Colico knot.

Narrow peaks with high-amplitude (H/V > 2) are generally found in the central part of the sections, while plateau-like peaks (H/V > 1.5) are evident close to the edge of the valley in section 1 (B_009 and B_012) and section 3 (station B_019, to South) in the Montecchi area and in section 4 (northernmost station B_002) in Valtellina.

On the other hand, small amplitude, smooth plateau-like peaks reflecting the likely fall of 1D condition (Guillier et al., 2006; Bonnefoy- Claudet et al., 2009), occur at the intermediate location across the transect; in particular, this behaviour is apparent (Fig. 6) from the recordings from stations along sections 1 (station B_010), 2 (station B_016) and 4 (station B_006). In these cases, the HVSR peaks are weak or poorly evident, as a consequence of 2D resonance effects or other unknown effects, and, therefore, the Vs-versus-depth profiles were not modelled at these locations.

4.2. Subsurface imaging

The subsurface seismic structure of the Montecchi-Colico area is shown with three HVSR pseudo-2D cross-sections (sections 1, 2 and 3, Fig. 2 and Fig. 6). Based on the results from the Teglio calibration site and on the additional information from the S02-S03 borehole logs (Fig. 2), the interface between the top of the seismic bedrock (metamorphic basement) and the overlaying valley-infill could be interpreted (Fig. 7).

In Section 3, in particular in Sub-section 3.1, several of the difficulties related to inversion of HVSR data have been recalled. In order to provide a rough, empirical assessment of the reliability of the results, the following procedure is applied to the HVSR data from pseudo 2-D section 2. For each of five stations (B_013, B_014, B_015, B_017, B_018), an ensemble of 2550 models considered by the DINVER modulo during the inversion procedure, are examined: both the HVSR modelled curve and the Vs-versus-depth curve are represented with colours which depend on the misfit between the modelled HVSR curve and the field data (Fig. 8, top and middle boxes). The uncertainty on the depths of the seismic bedrock, i.e., the discontinuity between the stiff valley infill and the underlying high-velocity basement, is determined by considering the models whose misfit is within the 10% of the difference between the minimum and maximum values among the 2550 models. The corre-
sponding interval of depths is drawn as a black bar in the drawings of Vs-versus-depth and in the cross-section shown in Fig. 8 (bottom box). This procedure is not designed to provide an absolute estimate of the uncertainty with a precise, rigorous statistical meaning, but is mostly aimed at showing the different reliability of the fits among various stations. Fig. 8 confirms the qualitatively plausible remark that the uncertainty is the greatest for HVSR curves which do not have a sharp peak at low frequencies (e.g., B_014 and B_015), whereas the smallest uncertainty is lower approximately by one fourth (e.g., B_013). Despite the remark that the estimated uncertainty does not have a rigorous statistical meaning, the uncertainty bars drawn on the cross-section in Fig. 8 support a sufficient reliability of the trend of the seismic bedrock along the cross-section. *4.3. Geological interpretation*

After calibration, the interpreted HVSR pseudo-2D sections represent an approximation of the shape of the paleo-valley floor. These results can be represented as a smoothed contour map of the elevation of the bedrock top (Fig. 9), by integration with the local geological and geomorphological constraints.

The top of the high-velocity seismic bedrock (V_S > 2600 m/s) was correlated with the surface geomorphology of the metamorphic basement rocks outcropping to the N (Montecchi) and to the S (Monte Legnone NW flank). The surface resulting from this interpretation portrays a SW-NE elongated, asymmetrical trough as deep as − 150 m below sea- level at station B_014 in section 2 (Fig. 9). Transverse profiles of this surface are irregular, with uplifted steps and counterscarps (Fig. 7).

The units with Vs lower than the seismic bedrock are interpreted as the sediment fill of the trough, in analogy with the comparable results at Teglio (violet and cyan colours in Figs. 4 and 7); their thickness might exceed 300 m, or even 400 m, at different stations. An upper, “low-velocity valley infill” layer shows some lateral variation of V_S in the range between 600 m/s and 1100 m/s (violet in Fig. 7). This Vs range may be indicative of some significant variation in the predominant type of the infill, from loose sedimentary deposits showing the lowest Vs to more consolidated and stiff sediments. The local boreholes provide additional information about this layer, being drilled through alluvial and lacustrine deposits down to at least 100 m b.g.s. A”high-velocity valley infill” layer with Vs ranging from 1200 m/s to 1600 m/s lays at places between these sediments and the bedrock (cyan colour in Fig. 7). It might be interpreted as dismembered rock masses, corresponding either to landslides or DSGSD collapsed bodies coming from the Mt. Legnoncino northern slope, in analogy with the observations at the calibration site of Teglio (De Franco et al., 2009). The underlying highest-Vs unit likely corresponds to the most continuous and homogeneous seismic bedrock of the area (pink colour in Fig. 7).

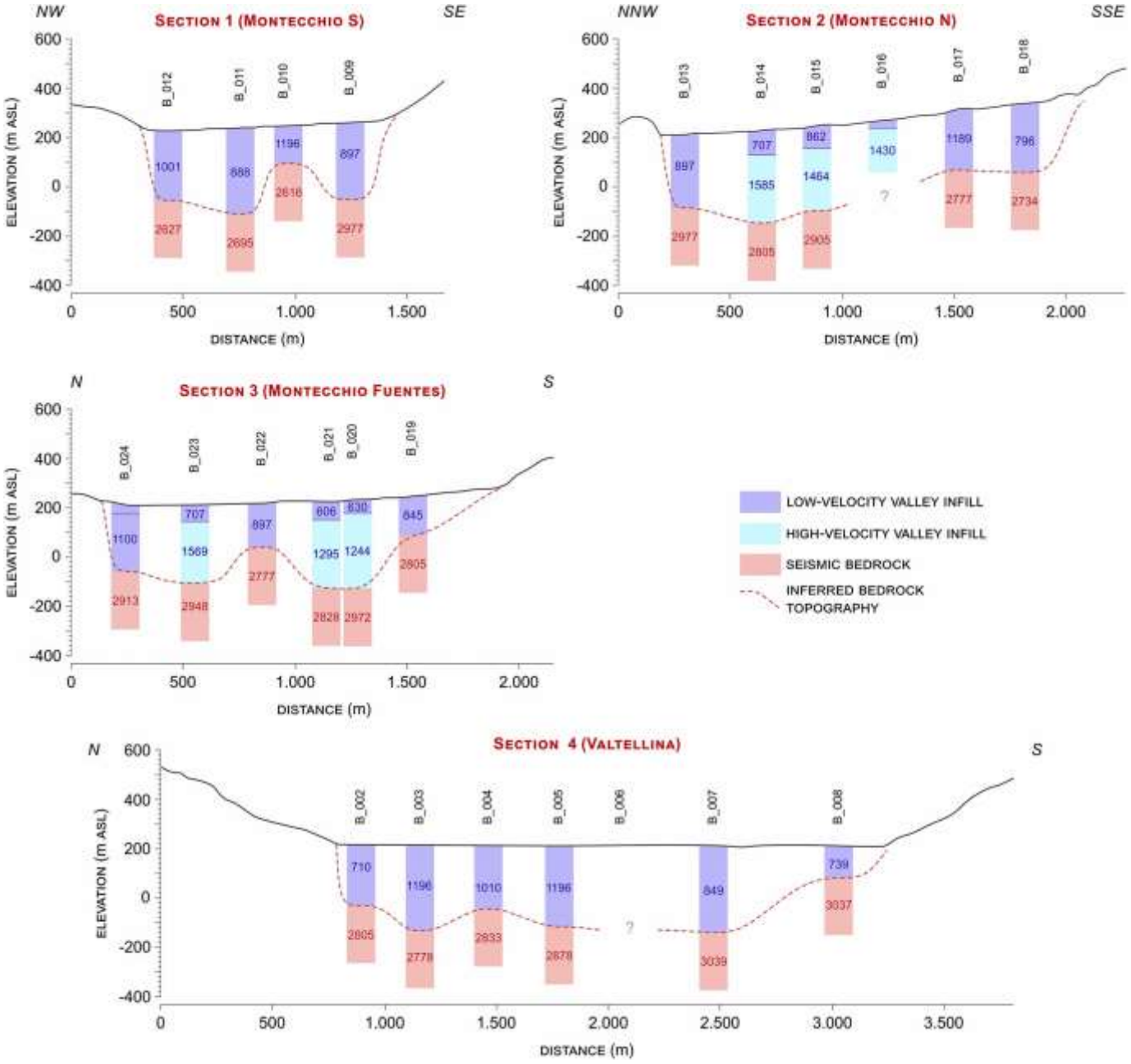

Fig. 7. HVSR pseudo-2D sections (location is shown in Fig. 2).

The subsurface structure of Valtellina is shown in HVSR section 4 (Fig. 7). The high-velocity seismic bedrock shows an asymmetrical trend and a wide and deep buried trough is clearly recognized.

The seismic bedrock elevation reaches − 230 m a.s.l. in the southern sector (station B_006 and B_007), where a steep flank may be correlated with the outcropping bedrock to the South. To the North, a double-step profile climbs up to the surface, apparently forming two separated plateaus at − 150 m a.s.l. and 0 m a.s.l. These results are in agreement with those found by Mele et al. (2012) in the central part of Valtellina (Ardenno-Postalesio, 25 km uphill in Valtellina from the study area), where an asymmetrical and N-stepped profile of the buried paleo-valley of Valtellina is traced.

The trough shown in section 4 is plausibly connected with the trough of the Montecchi-Colico area, as it is suggested by the contour map in Fig. 9. This interpretation is supported by the surface geomorphology. Comparing the maximum depths of the Valtellina trough (− 230 m a.s.l.) and the Montecchi-Colico trough (− 250 m a.s.l.), a slope of 0.004‰ to WSW could be estimated for this buried paleo-valley. Considering the depression that separates the relief of Montecchio North from the Montecchio di Fuentes (Fig. 2 and Fig. 9), a possible confluence between the ancient courses of the Mera and Adda rivers might be found in this position.

Differently from the Montecchi-Colico area, the upper seismic unit at Valtellina ("low velocity valley infill", violet in Fig. 7) shows a rather uniform V_S in the range between 700 m/s and 1200 m/s; low velocities are found in correspondence of the deepest trough (station B_007) and in the northern part, juxtaposed to the outcropping bedrock in the mountain slope (station B_002). In our interpretation, this structure is more simple than in the Montecchi-Colico transects, because the sedimentary infill of Valtellina directly covers the basement, without DSGSD-related rock masses in between. Accordingly, Fig. 2 and Fig. 9 show that section 4 runs between the tips of the DSGSD areas which characterize the Valtellina valley flanks.

Fig. 8. Top: Comparison between modelled and observed HVSR curves for an ensemble of 2550 models used during the inversion procedure with DINVER, for five stations along section 2. Middle: Vs-versus-depth profiles for the 2550 models, whose HVSR curves are shown in the top block. Bottom: Vertical pseudo 2-D section 2, showing the position of the seismic bedrock and of its uncertainty (black bar). In the top and middle blocks, the line colours correspond to the values of the misfit function; the white curves correspond to the best fit results. For each station, the uncertainty interval shown in the pseudo-2D section corresponds to the interval of depths obtained from the models whose fit differs from the best one by less than 10% of the difference between minimum and maximum value of the misfit function

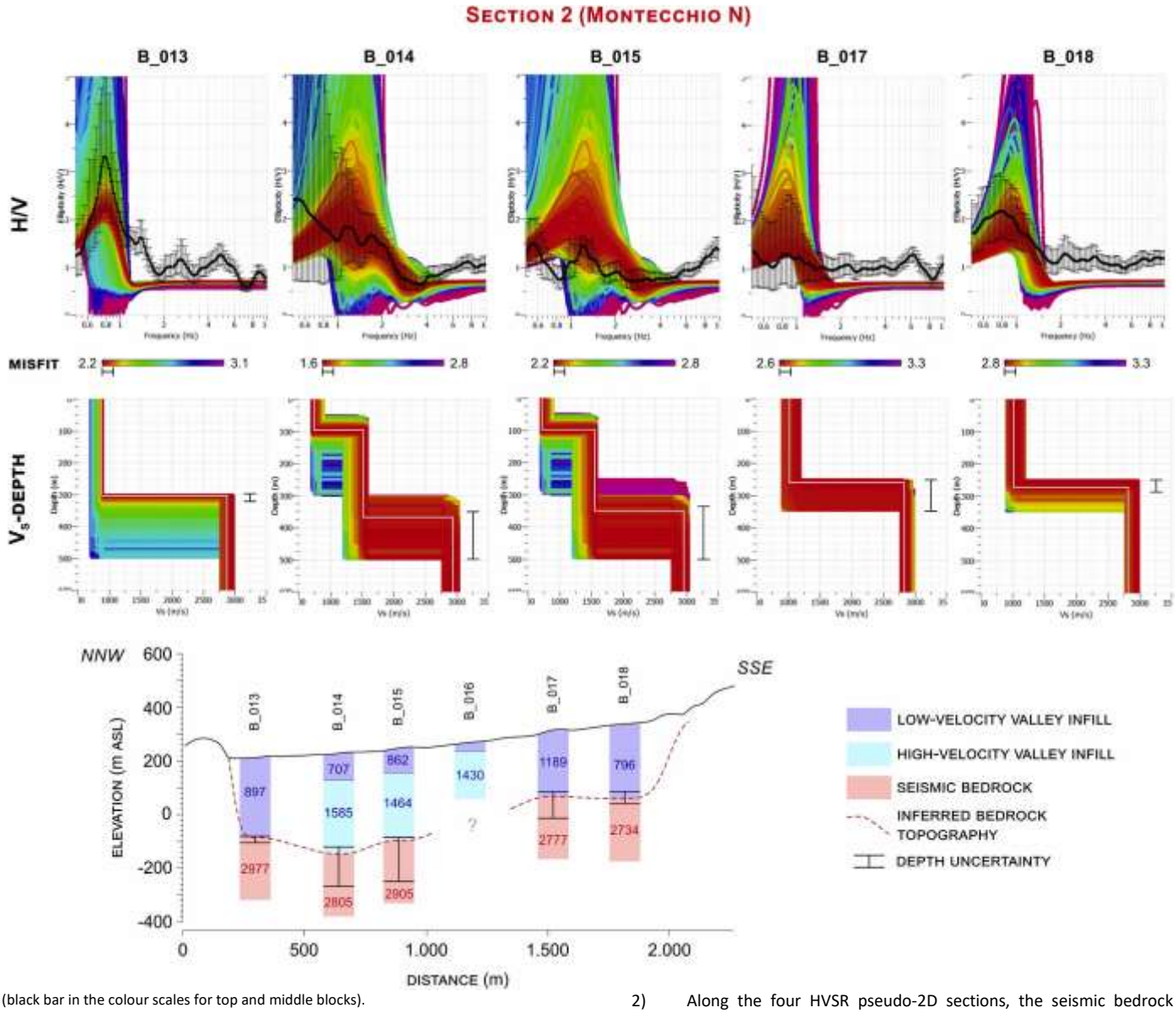

(black bar in the colour scales for top and middle blocks).

5. Conclusions

1) HVSR prospecting technique permitted to interpret the shape of the interface between the "seismic bedrock" (metamorphic basement) and the valley-filling sediments at the Colico knot. This was possible thanks to calibration of HVSR data with independent information from i) an analogue site in Valtellina, where Vs of the seismic units could be estimated from reflection seismic and calibrated to borehole data, and from ii) local borehole logs showing the lithotextures and depth of the valley-filling sediments down to some 100 m at the Colico knot, iii) integration with the surface geological and geomorphological constraints. The HVSR pseudo-2D sections of the bedrock top surface suggest that a SW-NE elongated buried trough, as deep as 250 m below sea- level and up to two-kilometer-wide, separates the NW slope of Mt. Legnoncino from the Piona – Montecchi crest line-up. This trough extends to the north-eastern side of the knot, where it prolongs below Pian di Spagna, reaching the present-day Adda Valley.

2) Along the four HVSR pseudo-2D sections, the seismic bedrock topography seems to be characterized by a buried stepped profile, with uplifted steps, plateaus and counterscarps that parallel the elongation of the trough and the regional NE-SW strike of the main foliation and of a mylonitic belt in the basement rocks. Along the central and south- western part of the trough, in the Montecchi – Piona bight sector, this shape corresponds to the interposition of an intermediate-Vs body, between the high-Vs seismic bedrock and the low-Vs sediments. Compared to the Teglio analogue, this body is here interpreted as a dismembered basement rock mass interposed between the seismic bedrock and the sediment fill of the trough. This pattern is interpreted as a plausible evidence of collapsing DSGSD from SE, i.e. from the NW slope of Mt. Legnoncino, where the mapped DSGSD reach the Lake Como shore (Fig. 2b and 9). This view suggests a control by DSGSD on the shape and evolution of the trough, coherently remarking that buried DSGSD are

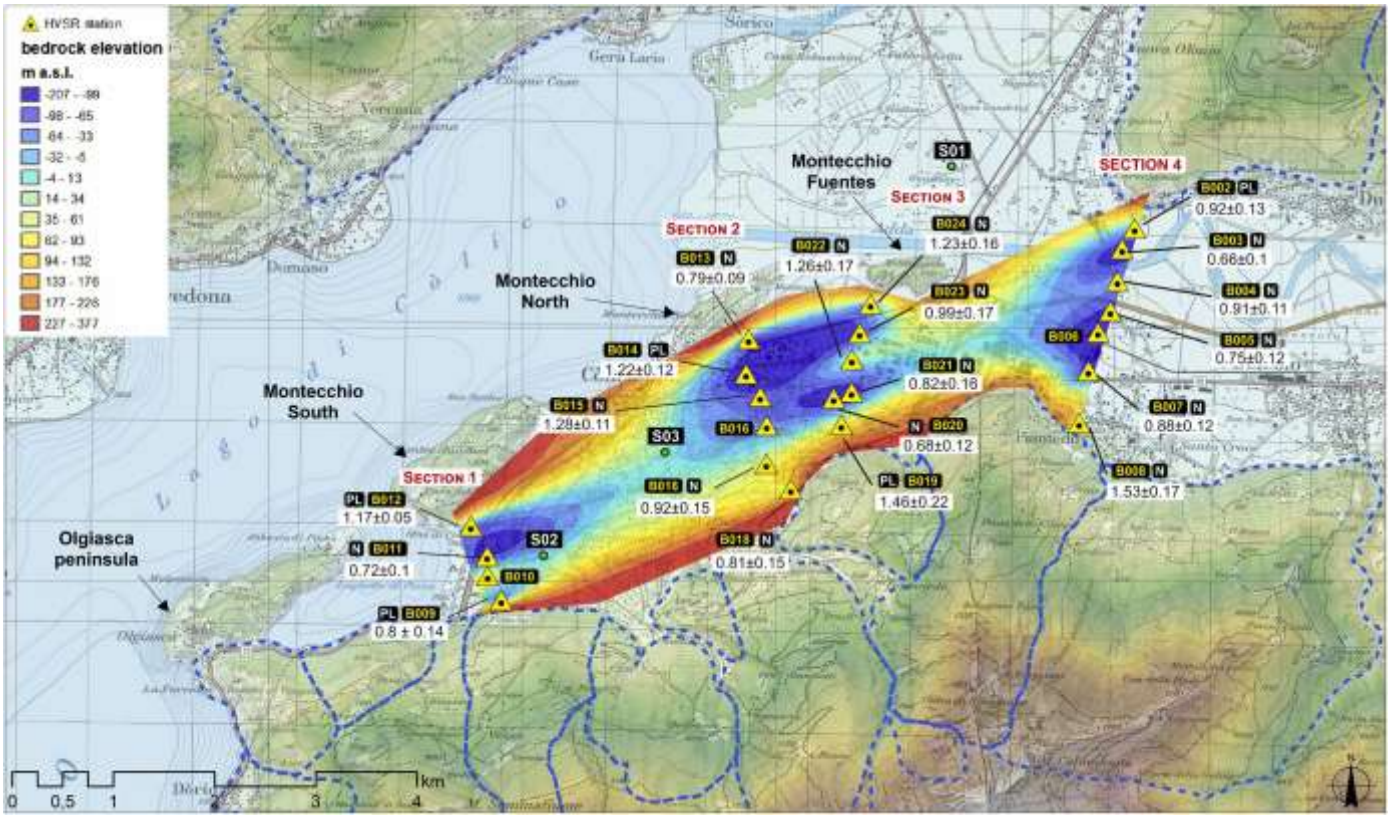

Fig. 9. Elevation map of the top of the seismic bedrock (in meters above mean sea level) in the Colico - Montecchi area. The f_0 frequency (in Hz) and the shape of the peak (N = narrow; PL = plateau-like) are reported. The boundaries of the DSGSD affecting the southern slopes are also redrawn in blue (compare with Fig. 2A and B).
(For interpretation of the references to colour in this figure legend, the reader is referred to the web version of this article.)

detectable by passive seismic profiling provided that a Vs-thickness calibration is available.

3) The evolution of the Colico knot was long and complex. Since the entrenchment of Lake Como depression (Messinian in literature), a watershed separated a paleo-Adda trough from the Mera valley. The modified remnants of this divide are represented by the present-day Piona-Montecchi-Mt.Foffricio line-up. Slope mobility, plausibly triggered by the structural grain and neotectonic/gravitative evolution, determined continuous modification of the landscape, leading to progressive filling and/or uplift of the troughs of the knot. We suggest that the (buried) paleo-Adda valley was progressively narrowed, uplifted and filled by the Mt. Legnoncino DSGSD until the confluence into Lake Como was locked, giving rise to the Piona bight. In this area the HVSR profiles suggest that some buried DSGSD-related features (the intermediate Vs rock masses) are plausibly sealed by the valley fill. At the surface, the cross-cut relations between DSGSD features and LGM deposits demonstrate that this evolution predates at least the LGM, but it is presumably much older than latest Quaternary. Glacial dynamics smoothed the valley slopes and the bedrock crest of the former Piona-Montecchi watershed, contributing to the recent diversion of the Adda river which started to build its delta into Lake Como after the LGM retreat.

4) The calibration with independent data is crucial for HVSR interpretation, both (a) to constrain the best fit of the HVSR peaks in terms of frequency and amplitude, and (b) to evaluate the strong lateral Vs variations that could affect the reliability of the 1-D assumption. Of course, besides the use of independent information, crucial steps to limit the ambiguity of 1D inversion and modelling and, eventually, to improve the interpretation of the results are i) a dense deployment of seismic stations across the survey area, ii) a proper processing of field data (see, e.g., Mi et al., 2019) and iii) an accurate inversion procedure considering the HVSR curves for individual and orthogonal horizontal directions and therefore anisotropic effects.

Declaration of Competing Interest None.

Acknowledgements

This work derives from an idea of Alfredo Bini, who suddenly passed away before its conclusion. We dedicate this paper to Alfredo, who was not only a co-Author but a Teacher for most of us, a humble and immense Scientist, the best Friend. The review by two anonymous Referees helped to ameliorate the manuscript.

References

Ambrosi, C., Crosta, G.B., 2006. Large sackung along major tectonic features in the Central Italian Alps. Eng. Geol. 83, 183–200. https://doi.org/10.1016/j.enggeo.2005.06.031.

Arai, H., Tokimatsu, K., 2004. S-wave velocity profiling by inversion of microtremor H/V spectrum. B. Seismol. Soc. Am. 94 (1), 53–63.

Bard, P.Y., Bouchon, M., 1985. The two-dimensional resonance of sediment-filled valleys. Bull. Seism. Soc. Am. 75, 519–541.

Barnaba, C., Marello, L., Vuan, A., Palmieri, F., Romanelli, M., Priolo, E., Braitenberg, C., 2010. The buried shape of an alpine valley from gravity surveys, seismic and ambient noise analysis. Geophys. J. Int. 180, 715–733. https://doi.org/10.1111/ j.1365-246X.2009.04428.x.

Bigi, G., Cosentino, D., Parotto, M., Sartori, D., Scandone, P., 1990. Structural model of Italy. Progetto Finalizzato Geodinamica CNR. Quad Ricerca Scientifica 114. SELCA (Firenze).

Bini, A., Cita, M.B., Gaetani, M., 1978. Southern Alpine lakes. Hypothesis of an erosional origin related to the Messinian entrenchment. Mar. Geol. 27, 271–288.

Bini, A., Chinaglia, N., Soldo, L., 1994. Stabilita dei versanti prospicienti la Penisola di` Olgiasca (Lago di Como Italia). Boll. Soc. Tic. Sci. Nat 82 (1), 41–56. Lugano.

Bonnefoy-Claudet, S., Cotton, F., Bard, P.-Y., 2006. The nature of noise wavefield and its applications for site effects studies: a literature review. Earth Sci. Rev. 79 (3–4), 205–227. https://doi.org/10.1016/j.earscirev.2006.07.004.

Bonnefoy-Claudet, S., Baize, S., Bonilla, L.F., Berge-Thierry, C., Pasten, C., Campos, J., Volant, P., Ferdugo, R., 2009. Site effect evaluation in the basin of Santiago de Chile using ambient noise measurements. Geophys. J. Int. 176, 925–937. https://doi.org/ 10.1111/j.1365-246X.2008.04020.x.

Borges, J.F., Silva, H.G., Torres, R.J.G., Caldeira, B., Bezzeghoud, M., Furtado, J.A., Carvalho, J., 2016. Inversion of ambient seismic noise HVSR to evaluate velocity and structural models of the lower Tagus Basin. Portugal. J. Seismol. 20 (3), 875–887. https://doi.org/10.1007/s10950-016-9564-x.

Castellaro, S., Mulargia, F., 2009. Vs30 estimates using constrained H/V measurements. Bull. Seism. Soc. Am. 99, 761–773. https://doi.org/10.1785/0120080179.

Castellaro, S., Mulargia, F., Bianconi, L., 2005. Passive seismic stratigraphy: a new efficient, fast and economic technique. J. Geotech. Environ. Geol. 3, 51–77.
Chinaglia, N., Soldo, L., 1994. Evoluzione del versante prospiciente la Penisola di Olgiasca (Lago di Como, Italia). In: Atti Terzo Convegno nazionale Giovani Ricercatori in Geologia Applicata (Potenza 1993). Geologia Applicata e Idrogeologia, XXVIII, 275–282, Roma, ISSN 0435–3870.
Ciancaleoni, L., Marquer, D., 2008. Late Oligocene to early Miocene lateral extrusion at the eastern border of the Lepontine Dome of the Central Alps (Bergell and Insubric areas, eastern Central Alps). Tectonics 27, TC4008.
Civico, R., Sapia, V., Di Giulio, G., Villani, F., Pucci, S., Baccheschi, P., Smedile, A., 2017. Geometry and evolution of a faultcontrolled Quaternary basin by means of TDEM and singlestation ambient vibration surveys: the example of the 2009 L'Aquila earthquake area. J. Geophys. Res.-Sol. Ea. 122, 2236–2259. https://doi.org/ 10.1002/2016JB013451.
D'Amico, V., Picozzi, M., Albarello, D., Naso, G., Tropenscovino, S., 2004. Quick estimate of soft sediments thickness from ambient noise horizontal to vertical spectral ratios: a case study in southern Italy. J. Earthq. Eng. 8 (6), 895–908.
D'Amico, V., Picozzi, M., Baliva, F., Albarello, D., 2008. Ambient Noise Measurements for preliminary Site-Effects Characterization in the Urban Area of Florence, Italy. B. Seismol. Soc. Am. 98 (3), 1373–1388.
De Franco, R., Biella, G., Caielli, G., Berra, F., Guglielmin, M., Lozej, A., Piccin, A., Sciunnach, D., 2009. Overview of high-resolution seismic prospecting in pre-Alpine and Alpine basins. Quarter. Int. 204 (1–2), 65–75. https://doi.org/10.1016/j. quaint.2009.02.011.
Fanetti, D., Anselmetti, F.S., Chapron, E., Sturm, M., Vezzoli, L., 2008. Megaturbidite deposits in the Holocene basin fill of Lake Como (Southern Alps, Italy). Palaeogeogr. Palaeocl. 259, 323–340. https://doi.org/10.1016/j.palaeo.2007.10.014.
Felber, M., Bini, A., 1997. Seismic survey in alpine and prealpine valleys of Ticino (Switzerland): evidence of a Late-Tertiary fluvial origin. Geologia Insubrica 2 (2), 46–67. ISSN 1429–9500.
Finckh, P.G., 1978. Are southern alpine lakes former Messinian canyons? Geophysical evidence for preglacial erosion in the southern alpine lakes. Mar. Geol 27 (3–4), 289–302.
Finckh, P., Kelts, K., Lambert, A., 1984. Seismic stratigraphy and bedrock forms in perialpine lakes. Bull. Geol. Soc. Am. 95, 1118–1128.
Foti, S., Parolai, S., Albarello, D., Picozzi, M., 2011. Application of Surface wave methods for seismic site characterization. Surv. Geophys. 32 (6), 777–825. https://doi.org/ 10.1007/s10712-011-9134-2.
Foti, S., Hollender, F., Garofalo, F., Albarello, D., Asten, M.W., Bard, P.-Y., Comina, C., Cornou, C., Cox, B., Di Giulio, G., et al., 2017. Guidelines for the good practice of surface wave analysis: a product of the InterPACIFIC project. Bull. Earthq. Eng. https://doi.org/10.1007/s10518-017-0206-7.
Geologische Karte der Schweiz 1:500.000, 2005. Geologische Bearbeitung durch: Institut für Geologie. Universitat Bern, und Bundesamt für Wasser und Geologie. ISBN: 3-¨ 906723-39-9.
Gosar, A., Lenart, A., 2010. Mapping the thickness of sediments in the Ljubljana Moor basin (Slovenia) using microtremors. B. Earthq. Eng. 8, 501–518. https://doi.org/ 10.1007/s10518-009-9115-8.
Gu´eguen, P., Cornou, C., Garambois, S., Banton, J., 2007. On the Limitation of the H/V Spectral Ratio using Seismic Noise as an Exploration Tool: Application to the Grenoble Valley (France), a Small Apex Ratio Basin. Pure Appl. Geophys. 164, 1–20. https://doi.org/10.1007/s00024-006-0151-x.
Guillier, B., Cornou, C., Krister, J., Moczo, P., Bonnefoy-Claudet, S., Bard, P.Y., Fah, D.,¨ 2006. Simulation of Seismic Ambient Vibrations: Does the H/V Provide Quantitative Information in 2D-3D Structures? In: Third International Symposium on the Effects of Surface Geology on Seismic Motion Grenoble, France, 2006 September 1–August 28, 185pp.
Gutenberg, B., 1958. Microseisms. Advances in Geophys. 5, 53–92.
Hinzen, K.G., Scherbaum, F., Weber, B., 2004. On the resolution of H/V measurements to determine sediment thickness, a case study across a normal fault in the lower Rhine embayment, Germany. J. Earthq. Eng. 8 (6), 909–926. https://doi.org/10.1142/ S136324690400178X.
Le Roux, O., Cornou, C., Jongmans, D., Schwartz, S., 2012. 1-D and 2-D resonances in an Alpine valley identified from ambient noise measurements and 3-D modelling. Geophysical Journal International 191 (2), 579–590. https://doi.org/10.1111/ j.1365-246X.2012.05635.x.
Lunedei, E., Albarello, D., 2010. Theoretical HVSR curves from full wavefield modelling of ambient vibrations in a weakly dissipative layered Earth. Geophys. J. Int. 181, 1093–1108.
Lunedei, E., Malischewsky, P., 2015. A review and some new issues on the theory of the H/V technique for ambient vibrations. In: Perspectives on European Earthquake Engineering and Seismology, Vol. 2. Springer International Publishing, Switzerland, pp. 371–394.
Mahajan, A.K., Praveen, K., 2018. Site characterisation in Kangra Valley (NW Himalaya, India) by inversion of H/V spectral ratio from ambient noise measurements and its validation by multichannel analysis of surface waves technique. Near Surf. Geophys 16 (3), 314–327. https://doi.org/10.3997/1873-0604.2018008.
Maheo, G., Gautheron, C., Leloup, P.H., Fox, M., Tassant-Got, L., Douville, E., 2013. Neogene exhumation history of the Bergell massif (southeast Central Alps). Terra Nova 25 (2), 110–118. https://doi.org/10.1111/ter.12013.
Mantovani, A., Valkaniotis, S., Rapti, D., Caputo, R., 2018. Mapping the palaeo-Piniada Valley, Central Greece, based on systematic microtremor analyses. Pure and Applied Geophysics 175 (3), 865–881. https://doi.org/10.1007/s00024-017-1731-7.
Mantovani, A., Zeid, N.A., Bignardi, S., Tarabusi, G., Santarato, G., Caputo, R., 2019. Seismic noise-based strategies for emphasizing recent tectonic activity and local site effects: the ferrara arc, Northern Italy, Case Study. Pure and Applied Geophysics 176 (6), 2321–2347. https://doi.org/10.1007/s00024-019-02120-8.
Maraio, S., Bruno, P.O.G.B., Picotti, V., Mair, V., Brardinoni, F., 2018. High-resolution seismic imaging of debris-flow fans, alluvial valley fills and hosting bedrock geometry in Vinschgau/Val Venosta, Eastern Italian Alps. J. of App. Geophys 157, 61–72. https://doi.org/10.1016/j.jappgeo.2018.07.001.
Martorana, R., Capizzi, P., D'Alessandro, A., Luzio, D., Di Stefano, P., Renda, P., Zarcone, G., 2017. Contribution of HVSR measures for seismic microzonation studies. Ann. Geophys-Italy 61 (2), SE225, 10.441/ag-7786.
Mele, M., Bini, A., Bassi, S., Giudici, M., Monti, M., Azzola, M., 2012. Single-Station Passive Seismic Stratigraphy for the characterization of subsurface structure of the Valtellina valley (Central Alps, northern Italy). EGU General Assembly Conference Abstracts, 2012.
Mi, B., Hu, Y., Xia, J., Socco, L.V., 2019. Estimation of horizontal-to-vertical spectral ratios (ellipticity) of Rayleigh waves from multistation active-seismic records. Geophy 84 (6). https://doi.org/10.1190/geo2018-0651.1.
Milano, P.F., Pennacchioni, G., Spalla, M.I., 1988. Alpine and pre-Alpine tectonics in the Central Orobic Alps (Southern Alps). Eclogae Geol. Helv. 81 (2), 273–293 (ISSN 0012-9402).
Milnes, A.G., Pfiffner, O.A., 1980. Tectonic evolution of the Central Alps in the cross section St Gallen-Como. Eclogae Geol. Helv. 73, 619–633.
Montrasio, A., et al., 1990. Carta Geologica della Lombardia in scala 1: 250.000. Servizio Geologico Nazionale, Regione Lombardia. Istituto Poligraficco e Zecca dello Stato (Roma).
Montrasio, A., Bersezio, R., Forcella, F., Jadoul, F., Sciesa, E., 1994. Geological interpretation of the profile CROP - Alpi Centrali (Passo Spluga-Bergamo). In: Montrasio, A., Sciesa, E. (Eds.), Proceedings Symposium CROP Alpi Centrali, Sondrio October 20–22, 1993, Quaderni di Geodinamica Alpina e Quaternaria, 2, 171–186, ISBN88–86596–00-6, Milano.
Mozco, P., Bard, P.-Y., 1993. Wave diffraction, amplification and differential motion near strong lateral discontinuities. Bull. seism. Soc. Am. 83 (1), 85–106.
Nakamura, Y., 1989. A method for dynamic characteristics estimation of subsurface using microtremor on the ground surface. Quarterly Report of RTRI 30, 25–33.
Nangeroni, G., 1971. Note geomorfologiche sul territorio montuoso comasco ad oriente del Lario. Atti Soc. Ital. Sci. Nat 115, 5–116 (Milano).
Nogoshi, M., Igarashi, T., 1971. On the amplitude characteristics of microtremors (part 2). Zisin J. seismSoc. Japan. 24, 26–40.
Oldenborger, G.A., Logan, C.E., Hinton, M.J., Pugin, A.M., Sapia, V., Sharpe, D.R., Russell, H.A.J., 2016. Bedrock mapping of buried valley networks using seismic reflection and air-borne electromagnetic data. J. Appl. Geophys 128, 191–201. https://doi.org/10.1016/j.jappgeo.2016.03.006.
Panzera, F., Romagnoli, G., Tortorici, G., D'Amico, S., Rizza, M., Catalano, S., 2019. Integrated use of ambient vibrations and geological methods for seismic microzonation. J. of Appl. Geophys. 170. https://doi.org/10.1016/j. jappgeo.2019.103820.
Paolucci, E., Albarello, D., D'Amico, S., Lunedei, Martelli L., Mucciarelli, M., Pileggi, D., 2015. A large scale ambient vibration survey in the area damaged by May-June 2012 seismic sequence in Emilia Romagna, Italy. Bull. of Earth. Eng. 13 (11), 3187–3206. Pedroncelli, A., 2013. Dinamica glaciale sulla cresta spartiacque tra Valtellina e Valchiavenna. In: Tesi di Laurea, Dipartimento Scienze della Terra. Universita degli` Studi di, Milano.
Pina-Flores, J., Perton, M., García-Jerez, A., Carmona, E., Luz˜ on, F., Molina-Villegas, J., ´ Sanchez-Sesma, F., 2016. The inversion of spectral ratio H/V in a layered system ´ using the diffuse field assumption (DFA). Geophys. J. Int. 208 (1), 577–588. https:// doi.org/10.1093/gji/ggw416.
Reynolds, J.M., 2011. An Introduction to Applied and Environmental Geophysics, 2nd edition. Wiley. 712 pp.
Roten, D., Fah, D., Cornou, C., Giardini, D., 2006. Two-dimensional resonances in Alpine ¨ valleys identified from ambient vibration wavefields. Geophys. J. Int. 165 (3), 889–905. https://doi.org/10.1111/j.1365-246X.2006.02935.x.
Schmid, S.M., Aebli, H.R., Heller, F., Zingg, A., 1989. The role of the Periadriatic Line in the tectonic evolution of the Alps. In: Coward, M.P., Dietrich, D., Park, R.G. (Eds.), Alpine Tectonics, Geological Society of London, Special Publications, 45, pp. 153–171. https://doi.org/10.1144/GSL.SP.1989.045.01.08.
SESAME, 2004. Guidelines for the implementation of the H/V spectral ratio technique on ambient vibrations. Measurements, processing and interpretation. SESAME European research project, WP12 – Deliverable D23.12. European Commission – Research General Directorate Project no. EVG1-CT-2000-00026 SESAME, 59 pp. http://sesame-fp5.obs.ujf-grenoble.fr/SES_TechnicalDoc.htm.
Spalla, M.I., Di Paola, S., Gosso, G., Siletto, G.B., Bistacchi, A., 2002. Mapping tectono-metamorphic histories in the lake Como basement (Southern Alps, Italy). Mem. Sci. Geol 54, 101–134 ((Padova), ISSN 0391-8602).
Tantardini, D., 2016. Geologia del Quaternario e geomorfologia della Bassa Valchiavenna. Ph.D. Thesis. Dipartimento Scienze della Terra, Universita degli Studi` di Milano.
Tarabusi, G., Caputo, R., 2017. The use of HVSR measurements for investigating buried tectonic structures: the Mirandola anticline, Northern Italy, as a case study. Int. J. Earth Sci 106 (1), 341–353. doi.org/10.1007/s00531-016-1322-3.
Tibaldi, A., Corazzato, C., 2001. Evidenze strutturali, litologiche e morfologiche di deformazioni recenti sul Monte Berlinghera (Lago di Mezzola, Alpi Centrali). In: Pasquare G. (Ed.), Tettonica recente e instabili` ta di versante nella Alpi Centrali,` 91–102, Fondazione Cariplo per la Ricerca Scientifica - CNR Istituto per la Dinamica dei Processi Ambientali, Milano (208 pp.).
Wathelet, M., 2006. Geopsy Software Manual. Technical Report, SESAME European Project.
Willett, S.D., Schlunegger, F., Picotti, V., 2006. Messinian climate change and erosional destruction of the central European Alps. Geology 34 (8), 613–616. https://doi.org/ 10.1130/G22280.1.
Yamanaka, H., Takemura, M., Ishida, H., Niwa, M., 1994. Characteristics of long-period microtremors and their applicability in exploration of deep sedimentary layers. Bull. seism. Soc. Am. 84, 1831–1841.